


DRAFT VERSION JULY 28, 2022

Typeset using L^AT_EX **modern** style in AAS_{TeX}631

Chemical Abundances for 25 JWST Exoplanet Host Stars with KeckSpec

ALEX S. POLANSKI ¹ IAN J. M. CROSSFIELD,¹ ANDREW W. HOWARD ²
HOWARD ISAACSON ^{3,4} AND MALENA RICE ^{5,6,*}

¹*Department of Physics and Astronomy, University of Kansas, Lawrence, KS 66045, USA*

²*California Institute of Technology, Pasadena, CA 91125, USA*

³*501 Campbell Hall, University of California at Berkeley, Berkeley, CA 94720, USA*

⁴*Centre for Astrophysics, University of Southern Queensland, Toowoomba, QLD, Australia*

⁵*Department of Physics and Kavli Institute for Astrophysics and Space Research, Massachusetts Institute of Technology, Cambridge, MA 02139, USA*

⁶*Department of Astronomy, Yale University, New Haven, CT 06511, USA*

Submitted to Research Notes of the AAS

ABSTRACT

Using a data-driven machine learning tool we report T_{eff} , $\log(g)$, $v \sin(i)$, and elemental abundances for 15 elements (C, N, O, Na, Mg, Al, Si, Ca, Ti, V, Cr, Mn, Fe, Ni, Y) for a sample of 25 exoplanet host stars targeted by JWST’s first year of observations. The chemical diversity of these stars show that, while a number of their companion planets may have formed in a disk with chemistry similar to Solar, some JWST targets likely experienced different disk compositions. This sample is part of a larger forthcoming catalog that will report homogeneous abundances of $\sim 4,500$ FGK stars derived from Keck/HIRES optical spectra.

Keywords: Abundance ratios (11), Chemical abundances (224), Metallicity (1031), Stellar abundances (1577), Exoplanets (498)

1. INTRODUCTION

The rapid rate of exoplanet discovery in the last two decades has been accompanied by a push to better understand the stars that host them. In particular, the effort to chemically characterize exoplanet hosts has led to a number of large catalogs reporting precise abundances of different elements (Adibekyan et al. 2012, Brewer et al. 2016, Clark et al. 2021). Refractory elements (Si, Fe, Mg) have especially been of interest due to their potential to break degeneracies in planet composition that arise from

Corresponding author: Alex S. Polanski

aspolanski@ku.edu

* 51 Pegasi b Fellow

knowledge of planet mass and radius alone. The ratios Fe/Si and Mg/Si can place constraints on the size of a rocky planet’s core or the composition of its mantle (Dorn et al. 2017, Unterborn & Panero 2017), while volatile abundances (C, N, O) enable comparisons of stellar to planetary C/O and N/O which can hint at the formation locations of gaseous planets (Öberg et al. 2011, Mordasini et al. 2016, MacDonald & Madhusudhan 2017). JWST has already begun to conduct its first observations of the atmospheres of other worlds, making a uniform determination of their host star abundances an important and timely step in the interpretation of those results (Pontoppidan et al. 2022).

2. SAMPLE & METHODS

We utilized **KeckSpec** to determine T_{eff} , $\log(g)$, $v \sin(i)$, and $[X/H]$ for 15 elements (Rice & Brewer 2020). **KeckSpec** is a version of the **Cannon** (Ness et al. 2015) designed for application on spectra from the High Resolution Echelle Spectrometer (HIRES, Vogt et al. 1994) on the Keck I telescope. The **Cannon** is a supervised learning algorithm that identifies correlations between the stellar parameters (“labels”) and the flux at every pixel in the stellar spectrum. A generative model is built using a set of stellar spectra with known stellar labels which can then be applied to determine labels for a new set of spectra. The **Cannon** has been effectively utilized to determine stellar parameters in a number of other surveys including APOGEE (Clark et al. 2021), RAVE (Casey et al. 2017), and LAMOST (Ho et al. 2017).

KeckSpec was trained on the SPOCS catalog (Valenti & Fischer 2005, Brewer et al. 2016) and therefore can only be applied to stars that are likely to reside in the parameter space spanned by that catalog (Rice & Brewer 2020, Table 3). Using HIRES spectra, we have employed **KeckSpec** to measure a homogeneous set of stellar abundances for 4,500 stars with $4700 < T_{\text{eff}} < 6600$ K (Polanski et al., *in prep*). Here we present our results for 25 planet-hosting dwarf stars targeted by JWST’s first year of observations. While some of our targets have abundances in the original SPOCS catalog we provide values from **KeckSpec** for completeness.

As discussed in Rice & Brewer 2020, **KeckSpec** displays a systematic offset that causes it to overestimate abundance values at low metallicity and underestimate them at high metallicity. This was attributed to a bias in the training sample whose labels were determined with **Spectroscopy Made Easy**. Using **KeckSpec** abundances for all the SPOCS catalog stars, we fit and correct for the offsets in each abundance value. This process is described in Polanski et al. (*in prep*), but across our sample the average correction for each element was slight: less than the scatter observed when comparing **KeckSpec** abundances to those of the SPOCS catalog. In Table 1 we provide the abundances for 15 elements along with T_{eff} , $\log(g)$, $v \sin(i)$, and signal to noise ratio (SNR/pixel) of the spectrum used. The average SNR of our spectra is ~ 200 , as determined using the median counts in a region centered on 5500 \AA ¹.

¹ Spectra available on request.

3. RESULTS & DISCUSSION

To assess the performance of **KeckSpec** on our sample, we compare the values we obtain for T_{eff} , $\log(g)$, $v \sin(i)$, and $[\text{Fe}/\text{H}]$ to those found through **SpecMatch** (**SM**) **Synthetic** (Petigura 2015). We find that the scatter in $\log(g)$, $v \sin(i)$, and $[\text{Fe}/\text{H}]$ to be 0.11, 1.1, and 0.05, respectively which are comparable to uncertainties returned by **SM**. For T_{eff} , the scatter is 65K which is nearly half the uncertainty quoted by **SM** underscoring the accuracy of our parameters.

We also compare the C/O and Mg/Si ratios derived from this work to the ones found by Kolecki & Wang (2021), who derived abundances for a JWST target sample that overlaps ours. Their analysis focused on 9 elements as opposed to our 15 and used a more heterogeneous data set whereas we use exclusively HIRES spectra. The average deviation between the two samples for Mg/Si is -0.07 which is within our uncertainties. For C/O, the difference is higher at -0.16, however, this disagreement is similar to what was found by Kolecki & Wang (2021) when comparing to values from SPOCS and is likely due to the fact that NLTE corrections were not applied in the SPOCS catalog.

The abundances obtained reveal that the systems targeted by JWST are chemically diverse, with abundances for most elements spanning an order of magnitude. Using abundance values for Ti, Ca, Mg, and Si, we calculate the α enhancement relative to iron and find that all stars in our sample, save HAT-P-26, are chemically consistent with being thin disk members. Mg/Si ratios for our sample range from WASP-121’s 0.85 to HD 182488’s 1.10 with a number of targets having $\text{Mg}/\text{Si} < 1$, suggesting that these stars could form “silicon-rich” companion worlds. Four targets, HAT-P-14 and WASP-17/18/121, form a distinct population in our sample with both low Mg/Si and C/O relative to the Sun. All of our JWST targets have C/O ratios below 0.8, with the highest being HD 189733 and WASP-69 at ~ 0.65 ².

Stellar abundances are an important piece of the planet composition puzzle, and comparisons with the atmospheric composition determination already being enabled by JWST in the coming months will be crucial to unveiling their formation histories.

² Figures visualizing these quantities and a CSV of Table 1 can be found at <https://aspolanski.github.io/jwst.html>

Table 1.

Name	T_{eff} ± 77	$\log(g)$ ± 0.09	$v \sin(i)$ ± 0.9	[C/H]	[N/H]	[O/H]	[Na/H]	[Mg/H]	[Al/H]	[Si/H]	[Ca/H]	[Ti/H]	[V/H]	[Cr/H]	[Mn/H]	[Fe/H]	[Ni/H]	[Y/H]	C/O	Mg/Si	SNR
HD 149026	5980	4.10	5.4	0.17	0.46	0.23	0.40	0.18	0.21	0.25	0.32	0.23	0.11	0.26	0.25	0.27	0.27	0.42	0.48 \pm 0.10	0.89 \pm 0.10	304
HD 15337	5131	4.43	0.9	0.06	0.08	0.06	0.15	0.13	0.15	0.12	0.10	0.11	0.11	0.11	0.14	0.12	0.13	-0.05	0.56 \pm 0.11	1.06 \pm 0.12	220
HD 182488	5365	4.42	2.0	0.10	0.21	0.16	0.15	0.12	0.15	0.09	0.13	0.12	0.13	0.13	0.20	0.14	0.14	0.07	0.48 \pm 0.10	1.11 \pm 0.13	265
HD 189733	5005	4.49	1.8	-0.12	-0.19	-0.21	-0.03	-0.04	-0.02	0.02	0.04	-0.01	-0.01	0.02	0.01	0.01	0.01	-0.13	0.67 \pm 0.14	0.92 \pm 0.11	328
HD 19467	5733	4.38	1.8	-0.03	-0.03	0.16	-0.15	-0.06	0.01	-0.05	-0.10	-0.02	-0.05	-0.16	-0.26	-0.14	-0.12	-0.09	0.36 \pm 0.07	1.02 \pm 0.12	302
HD 209458	6042	4.30	3.0	0.00	-0.01	0.13	-0.03	0.03	-0.03	0.03	0.08	0.06	0.04	0.05	-0.04	0.05	0.01	0.06	0.42 \pm 0.08	1.05 \pm 0.12	258
HD 75732	5258	4.42	0.7	0.25	0.54	0.30	0.50	0.29	0.36	0.28	0.27	0.27	0.28	0.29	0.42	0.30	0.37	0.18	0.50 \pm 0.10	1.08 \pm 0.13	320
HD 80606	5561	4.34	2.9	0.28	0.42	0.38	0.40	0.31	0.37	0.31	0.30	0.30	0.30	0.29	0.40	0.30	0.36	0.23	0.44 \pm 0.09	1.03 \pm 0.12	263
HD 22046	5060	4.54	1.9	-0.08	-0.24	-0.06	-0.14	-0.10	-0.10	-0.03	0.00	-0.04	-0.07	-0.01	-0.08	-0.03	-0.12	0.04	0.52 \pm 0.11	0.89 \pm 0.11	278
Kepler-51	5665	4.67	5.5	-0.07	-0.17	-0.10	-0.12	-0.11	-0.15	-0.05	0.03	-0.02	-0.05	-0.01	-0.08	-0.02	-0.14	0.06	0.59 \pm 0.12	0.92 \pm 0.11	27
HAT-P-14	6320	3.96	6.2	-0.15	0.15	0.22	-0.13	-0.08	-0.30	-0.02	0.04	0.06	-0.11	-0.02	-0.33	-0.02	-0.18	-0.04	0.24 \pm 0.05	0.91 \pm 0.12	208
HAT-P-1	5931	4.24	2.7	0.07	0.10	0.21	0.08	0.11	0.09	0.12	0.18	0.13	0.14	0.14	0.10	0.15	0.12	0.26	0.40 \pm 0.08	1.02 \pm 0.12	210
HAT-P-26	5011	4.39	2.1	0.11	-0.10	0.24	0.02	0.10	0.16	0.10	0.07	0.11	0.07	0.01	-0.03	0.02	0.03	-0.21	0.41 \pm 0.08	1.06 \pm 0.12	128
TOI-193	5392	4.36	2.5	0.19	0.30	0.22	0.33	0.23	0.29	0.24	0.22	0.22	0.22	0.22	0.33	0.24	0.29	0.08	0.52 \pm 0.11	1.03 \pm 0.13	83
TOI-421	5281	4.46	0.9	-0.01	-0.12	0.07	-0.06	0.01	0.04	-0.01	-0.02	0.02	0.02	-0.03	-0.08	-0.03	-0.04	-0.03	0.45 \pm 0.09	1.09 \pm 0.11	218
WASP-52	5089	4.46	4.1	0.16	0.29	0.13	0.42	0.19	0.23	0.26	0.32	0.22	0.23	0.26	0.37	0.29	0.28	0.12	0.59 \pm 0.12	0.90 \pm 0.10	120
WASP-121	6335	4.17	13.5	0.04	0.54	0.42	0.16	0.15	-0.03	0.24	0.25	0.22	0.01	0.23	0.17	0.24	0.17	0.29	0.23 \pm 0.05	0.85 \pm 0.12	204
WASP-127	5845	4.22	0.3	-0.12	-0.38	-0.01	-0.28	-0.15	-0.16	-0.15	-0.10	-0.08	-0.10	-0.16	-0.37	-0.16	-0.23	-0.17	0.43 \pm 0.09	1.04 \pm 0.11	210
WASP-166	6018	4.29	4.3	0.15	0.27	0.28	0.23	0.17	0.16	0.21	0.23	0.18	0.19	0.23	0.26	0.23	0.22	0.29	0.41 \pm 0.08	0.97 \pm 0.10	209
WASP-17	6490	4.08	6.4	-0.29	0.09	0.19	-0.08	-0.06	-0.36	0.00	0.05	0.07	-0.06	-0.02	-0.31	-0.00	-0.15	-0.08	0.18 \pm 0.04	0.91 \pm 0.10	170
WASP-18	6220	4.10	10.2	-0.01	0.22	0.37	0.08	0.05	-0.07	0.12	0.21	0.15	0.06	0.14	-0.01	0.15	0.03	0.19	0.23 \pm 0.05	0.88 \pm 0.12	203
WASP-39	5463	4.41	2.1	-0.04	-0.06	0.04	-0.02	-0.00	0.02	-0.01	-0.01	-0.00	0.00	-0.01	-0.03	-0.01	-0.03	0.02	0.46 \pm 0.09	1.06 \pm 0.13	149
WASP-63	5536	3.93	2.9	0.14	0.12	0.13	0.15	0.16	0.19	0.14	0.25	0.20	0.16	0.22	0.27	0.24	0.27	0.26	0.56 \pm 0.11	1.09 \pm 0.10	209
WASP-69	4876	4.50	2.6	0.27	0.38	0.18	0.68	0.33	0.39	0.40	0.44	0.32	0.31	0.35	0.50	0.41	0.45	0.21	0.67 \pm 0.14	0.88 \pm 0.12	237
WASP-77A	5569	4.45	3.7	-0.02	-0.05	0.06	-0.05	-0.00	0.00	-0.01	0.02	0.01	0.02	0.00	-0.02	0.01	-0.02	-0.00	0.46 \pm 0.09	1.07 \pm 0.10	211

NOTE— T_{eff} units: K; $\log(g)$ units: $[\text{cm s}^{-2}]$; $v \sin(i)$ units: km s^{-1} ; $[\text{X}/\text{H}]$ units: dex

REFERENCES

- Adibekyan, V. Z., Sousa, S. G., Santos, N. C., et al. 2012, *A&A*, 545, A32, doi: [10.1051/0004-6361/201219401](https://doi.org/10.1051/0004-6361/201219401)
- Brewer, J. M., Fischer, D. A., Valenti, J. A., & Piskunov, N. 2016, *ApJS*, 225, 32, doi: [10.3847/0067-0049/225/2/32](https://doi.org/10.3847/0067-0049/225/2/32)
- Casey, A. R., Hawkins, K., Hogg, D. W., et al. 2017, *ApJ*, 840, 59, doi: [10.3847/1538-4357/aa69c2](https://doi.org/10.3847/1538-4357/aa69c2)
- Clark, J. T., Clerté, M., Hinkel, N. R., et al. 2021, *MNRAS*, 504, 4968, doi: [10.1093/mnras/stab1052](https://doi.org/10.1093/mnras/stab1052)
- Dorn, C., Venturini, J., Khan, A., et al. 2017, *AAP*, 597, A37, doi: [10.1051/0004-6361/201628708](https://doi.org/10.1051/0004-6361/201628708)
- Ho, A. Y. Q., Ness, M. K., Hogg, D. W., et al. 2017, *ApJ*, 836, 5, doi: [10.3847/1538-4357/836/1/5](https://doi.org/10.3847/1538-4357/836/1/5)
- Kolecki, J. R., & Wang, J. 2021, arXiv e-prints, arXiv:2112.02031. <https://arxiv.org/abs/2112.02031>
- MacDonald, R. J., & Madhusudhan, N. 2017, *ApJL*, 850, L15, doi: [10.3847/2041-8213/aa97d4](https://doi.org/10.3847/2041-8213/aa97d4)
- Mordasini, C., van Boekel, R., Mollière, P., Henning, T., & Benneke, B. 2016, *ApJ*, 832, 41, doi: [10.3847/0004-637X/832/1/41](https://doi.org/10.3847/0004-637X/832/1/41)
- Ness, M., Hogg, D. W., Rix, H. W., Ho, A. Y. Q., & Zasowski, G. 2015, *ApJ*, 808, 16, doi: [10.1088/0004-637X/808/1/16](https://doi.org/10.1088/0004-637X/808/1/16)
- Öberg, K. I., Murray-Clay, R., & Bergin, E. A. 2011, *ApJ Letters*, 743, L16, doi: [10.1088/2041-8205/743/1/L16](https://doi.org/10.1088/2041-8205/743/1/L16)
- Petigura, E. A. 2015, PhD thesis, University of California, Berkeley, United States
- Pontoppidan, K., Blome, C., Braun, H., et al. 2022, arXiv e-prints, arXiv:2207.13067. <https://arxiv.org/abs/2207.13067>
- Rice, M., & Brewer, J. M. 2020, *ApJ*, 898, 119, doi: [10.3847/1538-4357/ab9f96](https://doi.org/10.3847/1538-4357/ab9f96)
- Untertorn, C. T., & Panero, W. R. 2017, *ApJ*, 845, 61, doi: [10.3847/1538-4357/aa7f79](https://doi.org/10.3847/1538-4357/aa7f79)
- Valenti, J. A., & Fischer, D. A. 2005, *ApJS*, 159, 141, doi: [10.1086/430500](https://doi.org/10.1086/430500)
- Vogt, S. S., Allen, S. L., Bigelow, B. C., et al. 1994, in *Society of Photo-Optical Instrumentation Engineers (SPIE) Conference Series*, Vol. 2198, Instrumentation in Astronomy VIII, ed. D. L. Crawford & E. R. Craine, 362, doi: [10.1117/12.176725](https://doi.org/10.1117/12.176725)